IEEE Access
Multidisciplinary | Rapid Review | Open Access Journal

Received April 10, 2019, accepted April 24, 2019, date of publication April 29, 2019, date of current version May 9, 2019.

Digital Object Identifier 10.1109/ACCESS.2019.2913704

Dynamic Thermal Analysis of High-Voltage Power Cable Insulation for Cable Dynamic Thermal Rating

PENG-YU WANG[1], HUI MA[2], (Senior Member, IEEE), GANG LIU[1], (Member, IEEE), ZHUO-ZHAN HAN[1], DE-MING GUO[1], TAO XU[3], AND LONG-YUN KANG[1]

[1]School of Electric Power, South China University of Technology, Guangzhou 510640, China
[2]School of Information Technology and Electrical Engineering, The University of Queensland, Brisbane, QLD 4072, Australia
[3]Transmission Management, Guangzhou Power Supply Co., Ltd., Guangzhou 510310, China

Corresponding author: Gang Liu (liugang@scut.edu.cn)

ABSTRACT Since cable insulation with low thermal conductivity occupies a large proportion of high-voltage cable, an optimization analysis on dynamic thermal behavior of cable insulation can be very useful to improve the accuracy of cable dynamic thermal rating. In this paper, the dynamic thermal analysis of cable insulation is carried out by combining the theoretical method and finite-element analysis (FEA) method. Based on the analysis, it is proved that using IEC recommended transient thermal model of cable insulation will bring certain error to cable dynamic temperature evaluation, especially at the early stage of cable temperature rise. Moreover, in this paper, an implementable optimization method for transient thermal model of cable insulation is developed. The improvement of the optimized model compared with the IEC model on cable dynamic thermal rating is verified by the FEA method. The results confirm that the optimized model can better model the dynamic thermal behavior of cable than the IEC model and the improvement is more obvious for dynamic thermal rating of cable with high voltage level and under large load. The methodology developed in this paper can pave a way for electricity utilities to increase cable utilization while still ensuring cable reliability.

INDEX TERMS Dynamic thermal analysis, ampacity, high voltage power cable, transient thermal model, optimization.

I. INTRODUCTION

With the continuous increase of electricity demand, utilities are facing an increasing challenge of maximizing the utilization of their high voltage cables while preventing overheating these cables. Thus, cable thermal analysis has attracted a lot of attention [1]–[2]. It is essential to accurately assess the cable ampacity, which is the maximum current that the cable conductor can carry yet within its allowable maximum temperature [3]–[4].

IEC 60287 has been widely adopted for cable ampacity calculation [5]–[6]. However, the calculation is under steady state and with the assumption that the worst case scenarios occur simultaneously [7]. Therefore, the ampacity calculated is rather conservative. Based on this calculation, the cable could be under-utilized for a significant portion of its service time. To increase the power flow of a cable while still maintain a satisfied safety margin, dynamic thermal rating methods are proposed [8]–[12]. These methods calculate the maximum conductor operating temperature on the basis of instantaneous cable loading and environment conditions [13]–[15].

The dynamic thermal rating methods require an accurate model of a cable's main components including its insulation [13]. However, the thermal resistance, thermal capacitance and temperature distribution of cable insulation are not linear with respect to its thickness. It is necessary to investigate the dynamic thermal behavior of cable insulation [7], [16]–[17].

In [16], the cable insulation was represented by a lumped π circuit. The insulation thermal capacitance was used to represent the total heat stored in the insulation. Part of the

The associate editor coordinating the review of this manuscript and approving it for publication was Kan Liu.

insulation thermal capacitance was placed at the cable conductor and other at the cable sheath with a certain ratio. This ratio is called Van Wormer coefficient, which is only determined by the cable structure and insulation radius. However, a steady state temperature distribution was assumed even for the transient conditions in [16]. This can bring errors and inaccuracies for the cable dynamic thermal rating. The above lumped π circuit and constant Van Wormer coefficient have been also adopted for the long-duration thermal transient calculation in IEC 60853 [18].

In [17], the thermal field distribution in the cable insulation was obtained by solving a homogeneous equation of heat conduction in conjunction with a set of simplified boundary conditions. However, the simplification of the boundary conditions may introduce some errors, which can accumulate to an undesirable level if the cable is under highly fluctuating load condition. To improve the accuracy in modeling the thermal transient behavior of cable insulation, in [7] the cable insulation was divided into several sections. Each section was represented by a lumped thermal circuit. However, the details of this method were not provided in [7].

In cable thermal dynamic rating, the lumped π thermal model and the constant Van Wormer coefficient recommended by IEC 60853 are used. However, the time-varying characteristic of Van Wormer coefficient during cable thermal transient and the influence of applying a constant Van Wormer coefficient to cable dynamic temperature evaluation have not been considered in detail and fully understood. Though some improved methods (e.g. [7]) for the lumped thermal model of cable insulation have been proposed, there still lacks an appropriate method for determining the number of insulation sections in practice.

In this paper, the Van Wormer coefficient is treated as a variable and determined based on the temperature transient distribution in cable insulation. An approximated solution for obtaining the time-varying Van Wormer coefficient is derived. An error analysis of temperature calculation by adopting the lumped π insulation thermal model as recommended by IEC 60853 is also conducted. Moreover, a new method of determining the proper number of insulation sections for an improved cable insulation thermal model is proposed. Furthermore, for different cable insulation thickness and cable load, the improvement in the accuracy of dynamic temperature evaluation through the use of the improved model is discussed. The theoretical derivations are validated by the finite element method (FEM) simulation.

An accurate and easy-to-use cable thermal model is crucial to the implementation of cable dynamic thermal rating schemes. The improved thermal model of cable insulation and calculation method proposed in this paper can be integrated into the existing real-time cable thermal rating systems to achieve the purpose of increasing the cable utilization while ensuring its reliability.

II. A BRIEF REVIEW OF FINITE ELEMENT METHOD AND THERMOELECTRIC EQUIVALENT METHOD FOR CABLE DYNAMIC THERMAL RATING

A. FINITE ELEMENT METHOD (FEM)

In this paper, FEM is used for cable temperature estimation and thermal model verification.

1) HEAT CONDUCTION EQUATION

For a cable section with a volume of V and surface area of A, the first law of thermodynamics is applicable as

$$\frac{dU}{dt} - Q_F - W = 0 \tag{1}$$

where t is the time, U is the intrinsic energy of the cable section, Q_F is the heat flow passing through its surface and W is the heating power of the cable section. It is assumed that any small change in the density of the cable material caused by the temperature variation can be ignored. Using Fourier's law and Gauss' integral theorem, (2) can be derived from (1)

$$\int_V \left[\rho c \frac{\partial \theta}{\partial t} - \mathrm{div}\,(\lambda \mathrm{grad}\theta) - P\right] \mathrm{d}V = 0 \tag{2}$$

where ρ, c, θ, λ and P denote the density, specific heat, temperature, heat conductivity coefficient and heating power density of the cable section. (2) can be written as

$$\rho c \frac{\partial \theta}{\partial t} = \mathrm{div}\,(\lambda \mathrm{grad}\theta) + P \tag{3}$$

Assuming the cable's material are temperature and time independent, the differential operator div $(\lambda \mathrm{grad}\theta)$ in (3) can be transformed to a Laplace operator $\lambda \Delta^2 \theta$. Since a cable's cross-sectional diameter is much smaller than its length, the heat flow in axial direction can be neglected. Thus, (3) can be reduced to a two-dimensional heat conduction as [19]

$$\frac{\partial \theta}{\partial t} = a\left(\frac{\partial^2 \theta}{\partial x^2} + \frac{\partial^2 \theta}{\partial y^2}\right) + \frac{P}{\rho c} \tag{4}$$

where $a = \lambda / c\rho$ is the thermal diffusivity [20].

2) BOUNDARY CONDITION EQUATIONS

In FEM modeling (5) defines the boundary temperature as a function of time and position, (6) defines the heat flux orthogonal to the boundary as a function of time and position and (7) defines the convective heat transfer coefficient and temperature of fluid at the boundary [20]

$$\theta_B(x, y)|_\Gamma = f_B(x, y)|_\Gamma \tag{5}$$

$$-\lambda \left.\frac{\partial \theta_B(x, y)}{\partial n}\right|_\Gamma = q_n(x, y)|_\Gamma \tag{6}$$

$$-\lambda \left.\frac{\partial \theta_B(x, y)}{\partial n}\right|_\Gamma = h\left[\theta_B(x, y) - \theta_F(x, y)\right]|_\Gamma \tag{7}$$

where Γ denotes the boundary, θ_B and θ_F are the temperature of solid and fluid at the boundary respectively, h is the convective heat transfer coefficient and λ is the heat conductivity coefficient of solid material.

TABLE 1. Parameters of the 110kV500mm² cable in modeling.

Structure	Diameter /mm	Specific heat /J·kg^{-1}·K^{-1}	Density /kg·m^{-3}	Thermal conductivity /W·m^{-1}·K^{-1}
Conductor	26.6	386	8920	401
Insulation	74.1	2526	1200	0.286
Metal sheath	84.6	917	2700	238
Jacket	92.6	2200	930	0.286

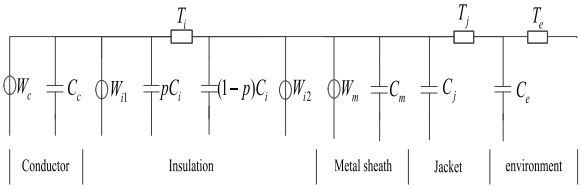

FIGURE 1. Lumped parameter thermal model. p - Van Wormer coefficient, W_c - joule heat of conductor, W_{i1} and W_{i2} - dielectric losses of insulation, W_m - screen losses of metal sheath, C_c,C_i, C_m, C_j, and C_e - thermal capacitance of conductor, insulation, metal sheath, jacket, and environment respectively, and T_i, T_j, and T_e - thermal resistance of insulation, jacket, and environment respectively.

B. THERMOELECTRIC EQUIVALENT (TEE) METHODS

In a TEE method, an equivalent thermal circuitry is obtained by replacing the electrical resistance, electrical capacitance and current source in the electric circuit with the thermal resistance, thermal capacitance and heat source respectively. The lumped parameter thermal model using TEE methods was adopted in [7], [21].

1) THERMAL MODEL

This paper is focused on thermal modeling for an unarmored single phase cable with copper conductor, XLPE insulation, aluminum sheath and MDPE jacket (refer to Table 1). With minor modifications, the methods developed in this paper can be applied to other types of cables.

A diagram of the lumped parameter thermal model is shown in Fig.1. Some simplifications can be made [7], [16]:

1) Since the insulation's thermal capacitance and temperature gradient is not linear along thickness, Van Wormer coefficient (p) is used to allocate part of the thermal capacitance to the conductor and other part to the metallic screen.
2) As the thermal conductivity of conductor and metal sheath is 2 to 3 orders higher than that of other components, the thermal resistance of conductor and metal sheath are ignored.
3) For simplification but without losing generality, some small components (i.e. semi-conductive layers) is either ignored or merged into cable insulation.

Note that the lumped parameter thermal model presented in Fig.1 is used for the transient calculation for a relatively long time duration, i.e. longer than one hour. For the transient calculation with time duration less than one hour, the other lumped parameter thermal model and the corresponding solution method such as the one detailed in IEC 60853-2 can be used [18]. The differences between the above two thermal models are the representation of insulation and the calculation method of Van Wormer coefficient.

This paper is focused on the lumped parameter thermal model for a long time duration. However, with some modifications, the methodologies and procedures for the long time duration model can be extended to the short time duration model. In the rest of this paper, the lumped parameter thermal model for the long time duration is referred to as the classical lumped parameter thermal model.

The differential equations that describe the relationship between the temperatures at different nodes and the circuitry parameters of Fig. 1 is

$$\begin{bmatrix} \dot{\theta}_j \\ \dot{\theta}_m \\ \dot{\theta}_c \end{bmatrix} = \begin{bmatrix} -\left(\frac{1}{C_4T_3}+\frac{1}{C_4T_4}\right) & \frac{1}{C_4T_3} & 0 \\ \frac{1}{C_3T_3} & -\left(\frac{1}{C_3T_1}+\frac{1}{C_3T_3}\right) & \frac{1}{C_3T_1} \\ 0 & \frac{1}{C_1T_1} & -\frac{1}{C_1T_1} \end{bmatrix} \cdot \begin{bmatrix} \theta_j \\ \theta_m \\ \theta_c \end{bmatrix} + \begin{bmatrix} \frac{1}{C_4T_4}\cdot\theta_e \\ \frac{1}{C_3}\cdot(W_m+W_{i2}) \\ \frac{1}{C_1}\cdot(W_c+W_{i1}) \end{bmatrix} \tag{8}$$

where θ_c, θ_m, θ_j and θ_e are the temperature of cable conductor, metal sheath, jacket and environment respectively and $C_1 = C_c + pC_i$, $C_3 = (1-p)C_i + C_m + C_j$, and $C_4 = C_e$. It is noted that θ_c, θ_m and θ_j are the temperatures at the terminals of the corresponding components. The analytical solution of (8) can be obtained by calculating the Eigen values and Eigen Vectors.

2) THERMAL PARAMETERS

In this paper, the cable power losses (W_c, W_{i1}, W_{i2} and W_m in Fig.1) are calculated using IEC 60287 [5]. The cable's screen losses can be ignored under certain conditions [7].

The equation for calculating thermal resistance and capacitance in Fig.1 can be found in [21]. The equation for calculating Van Wormer coefficient, p is [16], [18]

$$p = \frac{1}{2\ln\frac{r_i}{r_c}} - \frac{1}{\frac{r_i^2}{r_c^2}-1} \tag{9}$$

where r_c and r_i are the outer radius of conductor and insulation.

III. DISCUSSIONS ON THE CLASSICAL LUMPED PARAMETER THERMAL MODEL

In the classical lumped parameter thermal model shown in Fig 1, the temperature inside an object is treated as a one-dimensional function of time and is independent of location.

This is only valid when the internal temperature at different locations of the object is consistent at the same instant [17]. For a cable, its conductor and metal sheath have high thermal conductivity and can be regarded as isothermal. Its jacket has small thickness and the temperature difference between the inner and outer surfaces is insignificant. Thus, a cable's conductor, metal sheath, and jacket can be represented using a lumped parameter as in Fig.1.

However, the cable insulation has a very low thermal conductivity and it occupies a large proportion of the cable. Therefore, a large temperature gradient can exist along the insulation radial direction. The temperature variation in its spatial dimensions cannot be ignored in thermal modeling.

In the classical lumped parameter thermal model, the insulation thermal capacitance is placed part at the conductor and part at the metal screen according to the Van Wormer coefficient, p. To derive this coefficient, the steady state temperature distribution in the insulation is normally used.

However, since the actual insulation temperature is time-varying, the Van Wormer coefficient can be influenced by the temperature transient [7]. Thus, due to the use of steady state temperature in deriving Van Wormer coefficient, the classical lumped parameter thermal model can bring some errors and inaccuracies to the dynamic cable thermal rating.

The heat transfer in the environment around the cable is also a time varying process dependent on many factors. In the classical lumped parameter thermal model, representative environment condition is used. Some researchers proposed different approaches to consider the varying environmental condition [7], [13], [22]–[23]. However, in this paper the focus is on the thermal modeling of cable insulation. The thermal modeling of cable environment is beyond the scope of this paper.

IV. INVESTIGATION OF TIME-VARYING VAN WORMER COEFFICIENT AND ITS CALCULATION

A. PRELIMINARIES

Cable insulation of a unit length is taken for investigating the effects of the classical lumped thermal parameter model of insulation (Fig.1) on calculating cable temperature transient. For comparison, a distributed parameter thermal model of insulation is also established in this section.

Assume there is no heat flow along the cable axis direction, then a hollow cylindrical unit (Fig.2a) is adopted for establishing the distributed parameter thermal model of insulation. The first law of thermodynamics is applied to the cylindrical unit [20]

$$2\pi rc\rho \mathrm{d}r\frac{\mathrm{d}\theta}{\mathrm{d}t} = \mathrm{d}Q_i + W_i + 2\pi r\lambda\frac{\partial\theta}{\partial r} \tag{10}$$

where θ is temperature, r is the inner radius of the cylindrical unit, W_i is the losses of the cylindrical unit, $\mathrm{d}Q_i$ is the heat flowing into the cylindrical unit, ρ is the density and c is the specific heat. Assuming its thickness (i.e. $\mathrm{d}r$) is small enough, the cylindrical unit is isothermal. The lumped thermal model defined in (10) can be illustrated in Fig.2b.

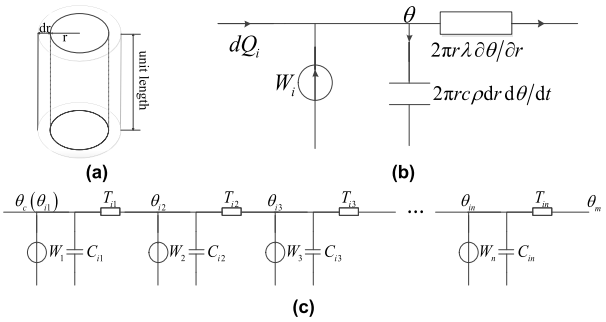

FIGURE 2. Distributed parameter thermal model of cable insulation (a) hollow cylindrical insulation unit; (b) lumped thermal parameter model of (a); (c) distributed parameter thermal model of insulation. $\theta_{i1}, \theta_{i2}, \ldots, \theta_{in}$ - temperature of each insulation unit, $T_{i1}, T_{i2}, \ldots, T_{in}$ - thermal resistance of each insulation unit, $C_{i1}, C_{i2}, \ldots, C_{in}$ - thermal capacitance of each insulation unit, and $W_1, W_2, \ldots, W_n$ - dielectric losses of each insulation unit. The footnotes c, m, and i stands for conductor, metal shield, and insulation respectively.

For two in-contact cylindrical units, the first law of thermodynamics is valid at their contact surface [20]. Thus, as shown in Fig.2c, a distributed parameter thermal model of insulation can be established by cascading all cylindrical units. These units are represented by their lumped thermal parameters. Note that for the distribution parameter thermal model of cable insulation, the number of units must be large enough.

The total heat absorbed by the thermal capacitances (pC_i and $(1\text{-}p)C_i$) of insulation in Fig. 1 is always equal to the total heat absorbed by all distributed thermal capacitances ($C_{i1}, C_{i2}, \ldots, C_{in}$) in Fig. 2c. With the definition of thermal capacitance, the below is held for any time instance [16]:

$$\begin{aligned} &pC_i\mathrm{d}\theta_c(t) + (1-p)\,C_i\mathrm{d}\theta_m(t) \\ &\quad = C_{i1}\mathrm{d}\theta_{i1}(t) + C_{i2}\mathrm{d}\theta_{i2}(t) + \ldots + C_{in}\mathrm{d}\theta_{in}(t) \end{aligned} \tag{11}$$

$$\mathrm{d}\theta_k(t) = \theta_k(t) - \theta_k(0) \tag{12}$$

It can be seen from (11) that Van Wormer coefficient, p is dependent on the temperature variation in insulation ($\mathrm{d}\theta_c(t)$, $\mathrm{d}\theta_m(t)$, $\mathrm{d}\theta_{i1}(t)$, …, $\mathrm{d}\theta_{in}(t)$). Note that footnotes c, m and i stand for conductor, metal shield and insulation respectively.

It is assumed the insulation is isothermal at $t = 0$ (corresponding to zero initial load). Using heat transfer theory [20], the radial temperature of the insulation over time can be obtained as shown in Fig.3. In Fig.3, the steady-state radial temperature distribution in insulation ($t = t_{\mathrm{state}}$) is only determined by the distribution of its thermal resistance [6].

From Fig.3 and (11), it can be inferred that Van Wormer coefficient p is time-varying during the cable insulation temperature rise. This is because during temperature rise, the temperature variation at different locations of the insulation are different. The above analysis is in agreement with [7].

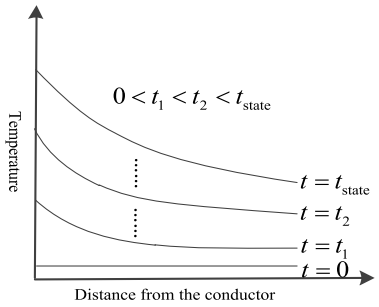

FIGURE 3. Radial temperature distribution in the cable's insulation at different time instants when insulation temperature is rising (assuming the insulation is isothermal at the initial time instant $t = 0$).

B. CALCULATION OF TIME-VARYING VAN WORMER COEFFICIENT

The Van Wormer coefficient p fluctuates with the rise of insulation temperature [7]. To study its changing trend, two extreme scenarios are considered: (1) $p = 1$, the insulation's thermal capacitance is allocated at the conductor; and (2) $p = 0$, thermal capacitance is allocated at the metallic screen.

When $p = 1$, (11) can be transformed to (13)

$$C_i' = C_{i1}\frac{\mathrm{d}\theta_{i1}(t)}{\mathrm{d}\theta_c(t)} + C_{i2}\frac{\mathrm{d}\theta_{i2}(t)}{\mathrm{d}\theta_c(t)} + \ldots + C_{in}\frac{\mathrm{d}\theta_{in}(t)}{\mathrm{d}\theta_c(t)} \tag{13}$$

where C_i' is the equivalent lumped parameter thermal capacitance of insulation for $p = 1$. Combining Fig.2c and Fig.3, the following equation is hold for $0 < t_i < t_{\text{state}}$,

$$\mathrm{d}\theta_c(t_i) = \mathrm{d}\theta_{i1}(t_i) > \mathrm{d}\theta_{i2}(t_i) > \ldots > \mathrm{d}\theta_{in}(t_i) > \mathrm{d}\theta_m(t_i) \tag{14}$$

From (13) and (14), we can have

$$C_i' < C_{i1} + C_{i2} + \ldots + C_{in} \tag{15}$$

It indicates C_i' is smaller than the lumped parameter thermal capacitance of insulation (i.e. the sum of $C_{i1}, C_{i2}, \ldots C_{in}$). In practice, the lumped parameter thermal capacitance of insulation is used to evaluate the transient temperature of cable. When the absorbed heat is the same, a larger lumped parameter thermal capacitance implies that the corresponding transient temperature variation is smaller [20]. Since (14) is established for the whole period of cable temperature rise, the error of the calculated transient temperature due to the use of $p = 1$ is always negative during this period.

When $p = 0$, (11) can be transformed to (16)

$$C_i'' = C_{i1}\frac{\mathrm{d}\theta_{i1}(t)}{\mathrm{d}\theta_m(t)} + C_{i2}\frac{\mathrm{d}\theta_{i2}(t)}{\mathrm{d}\theta_m(t)} + \ldots + C_{in}\frac{\mathrm{d}\theta_{in}(t)}{\mathrm{d}\theta_m(t)} \tag{16}$$

where C_i'' is the equivalent lumped parameter thermal capacitance for $p = 0$. For $0 < t_i < t_{\text{state}}$. From (14) and (16), we have

$$C_i'' > C_{i1} + C_{i2} + \ldots + C_{in} \tag{17}$$

It indicates that C_i'' is larger than the lumped parameter thermal capacitance insulation. It can be deducted that the error of the calculated transient temperature due to the use of $p = 0$ is always positive during this period.

In practice, there may have the situation that a cable's load suddenly increases when the cable operates in a steady-state. In such a situation, the insulation temperature rises faster at the position closer to the conductor. Thus, (14) is still valid and the two scenarios of $p = 1$ and $p = 0$ are also true.

The Van Wormer coefficient is in the range of $0 < p < 1$ [18]. A suitable coefficient should guarantee that its negative error (caused by the insulation thermal capacitance allocated at the conductor) equals to the positive error (caused by the insulation thermal capacitance allocated at the metallic screen). Correspondingly, the cable's transient temperature calculated from the distributed parameter thermal model equals to that calculated from the lumped parameter thermal model [16].

The heat absorbed by the lumped parameter thermal model of insulation, $Q'(t)$, can be described as [16]

$$\begin{aligned} Q'(t) &= pC_i\mathrm{d}\theta_c(t) + (1-p)\,C_i\mathrm{d}\theta_m(t) \\ &= pC_i'\mathrm{d}\theta_c(t) + (1-p)\,C_i''\mathrm{d}\theta_m(t) \\ &\quad + p(C_i - C_i')\,\mathrm{d}\theta_c(t) + (1-p)(C_i - C_i'')\,\mathrm{d}\theta_m(t) \end{aligned} \tag{18}$$

The heat absorbed by the distribution parameter thermal model of insulation, $Q(t)$, can be described as

$$Q(t) = C_{i1}\mathrm{d}\theta_{i1}(t) + C_{i2}\mathrm{d}\theta_{i2}(t) + \ldots + C_{in}\mathrm{d}\theta_{in}(t) \tag{19}$$

Substituting (13), (16) into (18) and (19), we can obtain the difference between $Q'(t)$ and $Q(t)$, $\Delta Q'(t)$ as

$$\begin{aligned} \Delta Q'(t) &= Q'(t) - Q(t) \\ &= p(C_i - C_i')\,\mathrm{d}\theta_c(t) + (1-p)(C_i - C_i'')\,\mathrm{d}\theta_m(t) \end{aligned} \tag{20}$$

Assuming the thermal capacitance of each insulation unit in the distribution parameter thermal model is equal, i.e. $C_{i1} = C_{i2} = \ldots = C_{in}$. Then (13) and (16) can be simplified as:

$$\begin{cases} C_i' = \dfrac{C_{in}}{\mathrm{d}\theta_c(t)}\displaystyle\sum_{j=1}^{n}\mathrm{d}\theta_{ij}(t) \\ C_i'' = \dfrac{C_{in}}{\mathrm{d}\theta_m(t)}\displaystyle\sum_{j=1}^{n}\mathrm{d}\theta_{ij}(t) \end{cases} \tag{21}$$

Accordingly, (20) can be written as

$$\begin{aligned} \Delta Q'(t) = pC_{in}&\left(n - \frac{1}{\mathrm{d}\theta_c(t)}\sum_{j=1}^{n}\mathrm{d}\theta_{ij}(t)\right)\mathrm{d}\theta_c(t) + (1-p)C_{in} \\ &\times\left(n - \frac{1}{\mathrm{d}\theta_m(t)}\sum_{j=1}^{n}\mathrm{d}\theta_{ij}(t)\right)\mathrm{d}\theta_m(t) \end{aligned} \tag{22}$$

Only when $\Delta Q'(t) = 0$, the two thermal models for insulation shown in Fig.1 and Fig.2c are equivalent at any time instance when temperature rises in insulation. Finally, the

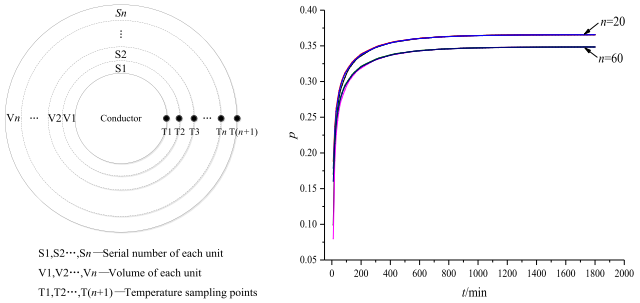

FIGURE 4. Calculated Van Wormer Coefficient $p(t)$ at different cable loading (a) temperature sampling points in FEM model; (b) results of $n = 20$ and $n = 60$, where n is the number of insulation units (sections).

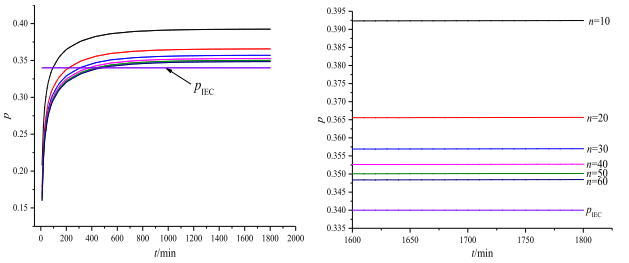

FIGURE 5. Calculated Van Wormer Coefficient $p(t)$ for different number of insulation units (a) results at 1200 A; (b) magnified view at steady state.

time-varying Van Wormer coefficient $p(t)$ can be derived from (22) as

$$p(t) = \frac{1}{n}\sum_{j=1}^{n}\frac{\mathrm{d}\theta_{ij}(t) - \mathrm{d}\theta_m(t)}{\mathrm{d}\theta_c(t) - \mathrm{d}\theta_m(t)} \tag{23}$$

To calculate $p(t)$, the temperature at any time instance at any location of the insulation should be known. However, this is difficult by using mathematical analytical methods [7], [17]. Therefore, FEM is used to calculate instantaneous temperature for the insulation. This is discussed in the next section.

V. RESULTS OF VAN WORMER COEFFICIENT P(T)

A. FEM MODELING SETUP

The cable modeled in this section is described in Table 1. Since the investigation is centered on the heat transfer inside the cable, it is assumed the cable is laid in uniform air and doesn't have neighboring cables.

Some simplifications of the cable structure in FEM model (Fig.4) are:

1) The stranded conductor is treated as a solid cylinder.
2) The conductor shield and insulation shield are merged into the insulation.
3) The equivalent radius is used to describe the corrugated aluminum sheath.

The cable losses can be calculated according to [5]. The boundary condition defined in (7) is applied to the cable surface (air temperature is set at 293.15 K). The convective heat transfer coefficient is determined according to the temperature difference between air and cable surface. The initial temperature of the cable is set to 298.15 K. The load duration is set to 30 hours to allow the cable to reach a steady state. The sampling interval is set to one minute.

B. APPROXIMATED SOLUTION OF VAN WORMER COEFFICIENT P(T)

To calculate $p(t)$ using (23), the total number of insulation units (i.e. n) should be large enough such that each unit can be regarded as isothermal. This requires a heavy computation. Thus, a finite value of n is adopted in this paper and the corresponding model is termed as approximated distributed parameter thermal model. With an increased number of insulation sections n, the above model can gradually provide an approximated solution to the distributed parameter thermal model [7]. To be consistent with the assumption that the thermal capacitance of each insulation unit is equal, the whole cable insulation is evenly divided into n units with each insulation unit has the same volume. With the temperature calculated from FEM, an approximated solution of (23) is obtained.

1) RESULTS OF P(T) AT DIFFERENT LOADING CONDITIONS

Three loading conditions of 800 A, 1000 A and 1200 A are considered. The insulation is divided into n units with equal volume as shown in Fig.4a. The temperature sampling point is on a unit's inner surface. Substituting temperature sampling points to (23), $p(t)$ is obtained. The results of $n = 20$ and $n = 60$ are shown in Fig.4b.

It can be seen that in both cases $p(t)$ under different loads are basically coincident. Therefore, the impact of cable loading on the calculation results of Van Wormer Coefficient p is negligible. In the following discussion in this section, the cable load is always set to 1200 A.

2) RESULTS OF P(T) AT DIFFERENT NUMBER OF INSULATION UNITS

The number of insulation units is set to $n = 10, 20, \ldots, 60$ and corresponding $p(t)$ are shown in Fig.5. In the figure, the IEC recommended p (i.e. p_{IEC}) is also provided for comparison. It is calculated by (9) and equals to 0.340 for the 110 kV 500 mm^2 cable in Table 1.

It can be observed from Fig. 5a that at the initial stage of temperature rise, $p(t)$ obtained by the approximated solution is much less than p_{IEC}. This can be explained as follows. At the initial stage, the temperature change at the inner surface of cable insulation is much larger than that at the outer surface of insulation. To offset the excess heat absorbed by the thermal capacitance of insulation concentrating at the conductor, more thermal capacitance of insulation should be allocated to the metallic screen, i.e. reducing p.

To verify the above analysis, an extreme scenario is considered here. Assuming a current is applied to the cable for a few milliseconds. Due to the large thermal resistance and

capacitance of insulation, the heat generated by the cable conductor cannot reach much depth of the insulation [20]. Only the insulation unit close to the conductor has temperature response at this moment. This can be expressed as

$$\mathrm{d}\theta_c = \mathrm{d}\theta_{i1} >> \mathrm{d}\theta_{ij} \approx 0 \ (j = 2, 3 \ldots n) \tag{24}$$

From (24), we have

$$\begin{cases} \dfrac{\mathrm{d}\theta_c - \mathrm{d}\theta_{ij}}{\mathrm{d}\theta_c - \mathrm{d}\theta_m} = \dfrac{1 - \dfrac{\mathrm{d}\theta_{ij}}{\mathrm{d}\theta_c}}{1 - \dfrac{\mathrm{d}\theta_m}{\mathrm{d}\theta_c}} \approx 1 \ (j = 2, 3 \ldots n) \\ p = \dfrac{1}{n}\sum_{j=1}^{n} \dfrac{\mathrm{d}\theta_{ij} - \mathrm{d}\theta_m}{\mathrm{d}\theta_c - \mathrm{d}\theta_m} = \dfrac{1}{n}\sum_{j=1}^{n}\left(1 - \dfrac{\mathrm{d}\theta_c - \mathrm{d}\theta_{ij}}{\mathrm{d}\theta_c - \mathrm{d}\theta_m}\right) \approx \dfrac{1}{n} \end{cases} \tag{25}$$

It can be seen that after applying current to the cable for a few milliseconds, p tends to be $1/n$. For the distributed parameter thermal model of insulation, the value of n approaches infinity. As a result, the value of p is close to zero. Note that this is the value, which makes the results of the lumped parameter thermal model and the results of distributed parameter thermal model equal for heat absorption process.

At the steady-state as shown in Fig.5b, p is larger than p_{IEC}. At this stage, the heat allocation in the insulation satisfies [16]

$$pC_i\,\theta_c|_{t=t_{state}} + (1-p)\,C_i\,\theta_m|_{t=t_{state}} = c_i \int_{r_c}^{r_i} 2\pi r\,\theta\,(r)|_{t=t_{state}}\,\mathrm{d}r \tag{26}$$

where $\theta_c|_t = tstate$ and $\theta_m|_t = tstate$ are conductor and metal sheath temperature at the steady state respectively, c_i is the specific heat of the insulation and $\theta(r)|_t = tstate$ denotes the function of temperature distribution along the radius of cable insulation. For the distributed parameter thermal model, $\theta(r)|_t = tstate$ has been depicted in Fig.3.

In the approximated distributed parameter thermal model, the total number of insulation units is finite. In each unit the internal temperature is replaced by the inner surface temperature. Thus, the temperature distribution function of the approximated model, $\theta'(r)|_t = tstate$ can be represented by a series of step functions. A comparison between the above two functions of temperature distribution is shown in Fig.6.

From Fig.6 it can be found that $\theta(r)|_t = tstate$ does not exceed $\theta'(r)|_t = tstate$ at each location of the insulation. So we have

$$c_i \int_{r_c}^{r_i} 2\pi r\,\theta\text{'}\,(r)|_{t=t_{state}}\,\mathrm{d}r > c_i \int_{r_c}^{r_i} 2\pi r\,\theta\,(r)|_{t=t_{state}}\,\mathrm{d}r \tag{27}$$

In (26), since $\theta_c|_{t=tstate}$ is larger than $\theta_m|_{t=tstate}$, p is positively correlated to right side of the equation. Combining (26) and (27), it can be found p calculated by (23) using a finite n (i.e. the result of the approximated solution method of p) is larger than p_{IEC} at the steady state.

From Fig.6, it can be also found that the two curves of $\theta(r)|_t = tstate$ and $\theta'(r)|_t = tstate$ approach each other with the increase of n. They will overlap when n approaches infinity. Therefore, p calculated by (23) at the steady state using infinite n is the same as p_{IEC}. p_{IEC} can be regarded as the true value of p at the steady state.

TABLE 2. Comparison of calculated p at steady state under different *n*.

	n=10	n=20	n=30	n=40	n=50	n=60	IEC
t=1800min	0.392	0.366	0.357	0.353	0.350	0.348	0.340

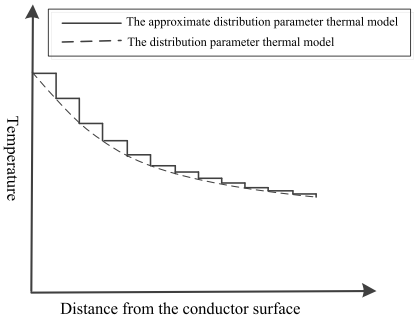

FIGURE 6. Radial temperature distribution function of the approximated parameter thermal model and that of the distributed parameter thermal model.

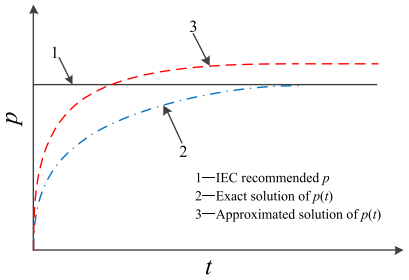

FIGURE 7. Van Wormer Coefficient obtained by different methods.

To investigate the effect of the value of n on the accuracy of p obtained from the approximated solution, the calculated p at steady state under different n are shown in Table 2. It can be seen from Table 2 and Fig.5a that: (1) when $n \leq 30$, an increase of n can improve the accuracy of p; (2) after $n = 30$, the improvement of the accuracy is insignificant. Therefore, an appropriate n can be determined based on the requirement on the accuracy of temperature calculation.

C. DISCUSSION

The trend of the exact solution of $p(t)$ (obtained when n approaches infinity in the approximated solution) is shown in Fig.7. In Fig.7, the IEC recommended p and the approximated solution of $p(t)$ are also presented.

It can be observed from Fig.7 that before the cable reaches steady state, the IEC recommended p and the approximated solution of $p(t)$ are both larger than the exact solution of $p(t)$. Recalled that the exact allocation for the thermal capacitance of insulation in the lumped parameter thermal model, a larger p means more thermal capacitance of insulation is allocated to the conductor. Section IV has pointed out that the thermal capacitance of insulation concentrating at the conductor

brings negative error to the dynamic temperature evaluation for cable. Therefore, adopting either the IEC recommended p or the approximated solution of $p(t)$ will bring negative error to the dynamic temperature evaluation of cable. Especially, for the IEC recommended p, at the early stage of cable temperature rise, a large error will be expected due to a large difference of p with respect to the exact solution.

VI. AN OPTIMIZATION METHOD FOR IMPROVING THE CLASSICAL LUMPED PARAMETER THERMAL MODEL

As discussed in the previous section, the adoption of a constant value of Van Wormer coefficient, p in the classical lumped parameter thermal model inevitably brings errors to the dynamic temperature evaluation of cable, especially at the early stage of temperature rise. A remedy is to divide the insulation into a number of sections (units) [7]. In this section, a similar approach is adopted and named as the optimized lumped parameter thermal model of insulation. Note that the implementation of the optimized lumped thermal model can be made on the basis of the classical lumped thermal model with some modifications. Compared to the implementation of the classical model, the insulation section number is the only additional parameter needed for implementing the optimized model.

A method for properly selecting insulation section number n for the optimized model is proposed in this section. An optimal n makes the difference of the temperature obtained from the distributed parameter thermal model and the optimized lumped parameter thermal model within an acceptable range. It can be reflected by the difference between the values of p obtained from the two models.

As mentioned in Section V, at the steady state p constantly approaches to the IEC recommended value with the increase of n. Therefore, the difference between the p_i (corresponding to n_i) calculated by (23) at the steady state and p_{IEC} is chosen as the criterion in determining the optimal value of n. When the difference satisfies (28), n_i can be regarded as the optimal number of insulation sections.

$$p_i - p_{\mathrm{IEC}} \le k \cdot p_{\mathrm{IEC}} \tag{28}$$

where k is a positive correction factor and decided according to the required accuracy of the temperature calculations.

At the state steady, (23) can be converted to (29). Based on the equation of thermal resistance for hollow cylinder, (30) can be derived [21].

$$p|_{t=t_{state}} = \frac{1}{n}\sum_{j=1}^{n}\frac{\theta_{ij}|_{t=t_{state}} - \theta_m|_{t=t_{state}}}{\theta_c|_{t=t_{state}} - \theta_m|_{t=t_{state}}} \tag{29}$$

$$\theta_{ij}|_{t=t_{state}} - \theta_m|_{t=t_{state}} = q \cdot \frac{1}{2\pi\lambda_i}\ln\frac{r_i}{r_{i(j-1)}} \tag{30}$$

In (30), q is the heat flow through insulation, $\lambda_i$is the heat conductivity coefficient of insulation, and r_{ij} ($j = 1, 2, \ldots n$) is the outer radius of insulation unit j (refer to Fig.4a). r_{i0} is equal to r_c. Since each insulation unit has the same volume, r_{ij} is

$$r_{ij}^2 = r_c^2 + j\frac{r_i^2 - r_c^2}{n} \tag{31}$$

Substitute (30) and (31) into (29), then the value of p at the steady state can be expressed as a function of only n, r_c and r_i

$$p|_{t=t_{state}} = \frac{1}{n\ln\frac{r_i}{r_c}}\sum_{j=1}^{n}\ln\frac{r_i}{\sqrt{r_c^2 + (j-1)\frac{r_i^2 - r_c^2}{n}}} \tag{32}$$

Combining (9), (28) and (32), a formula to determine the appropriate number of insulation unit can be obtained as

$$\frac{1}{n_i\ln\frac{r_i}{r_c}}\sum_{j=1}^{n_i}\ln\frac{r_i}{\sqrt{r_c^2 + (j-1)\frac{r_i^2 - r_c^2}{n_i}}} \le (1+k)\cdot\left(\frac{1}{2\ln\frac{r_i}{r_c}} - \frac{1}{\frac{r_i^2}{r_c^2} - 1}\right) \tag{33}$$

VII. VERIFICATIONS OF THE OPTIMIZED CLASSICAL LUMPED PARAMETER THERMAL MODEL

To estimate the dynamic temperature evolution of cable, the real-time data of the cable current and surface temperature are used [21], [24]. For simplification, in this section the end point of thermal models is set to the cable surface.

A. VERIFICATION BY FEM

The optimized lumped parameter thermal model of cable insulation developed in Section VI is verified by FEM method. The FEM was used to obtain dynamic temperatures of cable components including: (1) the conductor temperature, which is used for comparing the results obtained from the classical model and optimized model; and (2) the surface temperature, which is used as the input of both models.

To investigate the influence of insulation thickness and cable loading on the accuracy of the classical model and the optimized model, cables with different loading conditions and voltage levels (reflecting insulation thickness) were studied in FEM. The structural parameters of these cables are presented in Table 3. The thermal parameters of these cables are the same as that presented in Table 1.

The value of k in (33) was set to 0.05. With reference to Table 3, the optimal number of insulation sections were calculated as 29, 30 and 30 for 110 kV, 220 kV and 500 kV cables respectively.

TABLE 3. Structural parameters of cables with different voltage levels.

Voltage level	110 kV	220 kV	500 kV
Conductor	21.3mm	21.3mm	30.9mm
Insulation	48.9mm	58.1mm	74.1mm
Metal sheath	51.2mm	60.7mm	77.7mm
Jacket	56.2mm	65.7mm	85.4mm

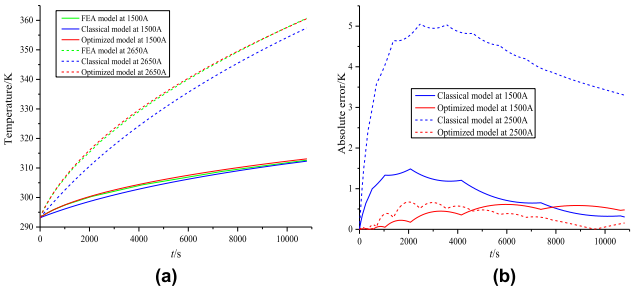

FIGURE 8. 110 kV cable thermal rating under different loads (a) conductor temperature calculated by optimized lumped thermal model, classical lumped thermal model, and FEM; (b) comparison of calculation errors with respect to FEM results.

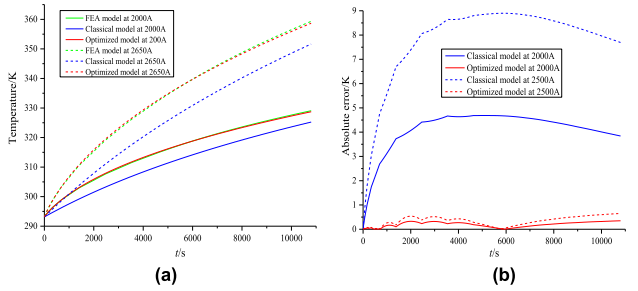

FIGURE 9. 220 kV cable thermal rating under different loads (a) conductor temperature calculated by optimized lumped thermal model, classical lumped thermal model, and FEM; (b) comparison of calculation errors with respect to FEM results.

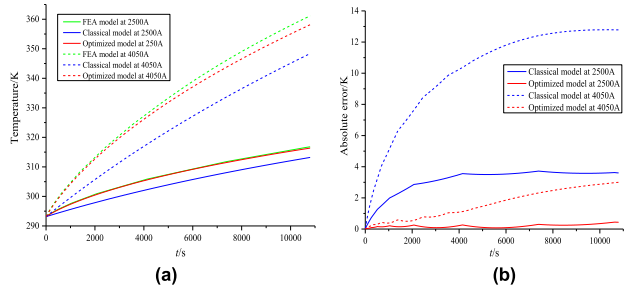

FIGURE 10. 500 kV cable thermal rating under different loads (a) conductor temperature calculated by optimized lumped thermal model, classical lumped thermal model, and FEM; (b) comparison of calculation errors with respect to FEM results.

The comparisons of the conductor temperature profiles under different load obtained from the classical model, the optimized model and FEM for 110 kV, 220 kV and 500 kV cables are presented in Fig.8a, Fig.9a and Fig.10a. The accuracies of the classical and optimized models with respect to FEM are shown in Fig.8b, Fig.9b and Fig.10b. In the simulations, all cables were subjected to a step load with a 3 hour duration.

As can be seen from Fig.8, Fig.9 and Fig.10, the classical model is not sufficiently accurate for modeling the dynamic thermal behavior of cables. The cable conductor temperatures calculated by the classical model under different loads are always lower than that calculated by FEM. This is also consistent with the analysis in the previous sections in this paper. A lower conductor temperature implies a large room for further increasing cable load. Thus, using the classical lumped thermal model to rate the dynamic ampacity of a cable may overheat the cable.

From Fig.8, Fig.9 and Fig.10, it can be also seen that compared to the conductor temperature profiles obtained from the classical model, the conductor temperature profiles obtained from the optimized model are closer to that obtained from FEM. For most of time instances, the absolute error of the optimized model is less than that of the classical model. Therefore, the optimized model can better model the dynamic thermal behavior of the cables than the classical model.

To investigate the influence of cable insulation thickness and cable load on the accuracy of the classical model and the optimized model, the maximum absolute errors and the averaged absolute errors of the conductor temperature obtained from the both models are presented in Table 4 and Table 5 respectively.

It can be seen from Table 4 and Table 5 that for cables with different voltage levels and under different loads, θ_{oe} and $\Delta\theta_{oe}$ (the maximum absolute error and averaged absolute error of the conductor temperature calculated by the optimized model respectively) are always smaller than corresponding θ_{oe} and $\Delta\theta_{ce}$ (the maximum absolute error and averaged absolute error of the conductor temperature calculated by the classical model respectively).

TABLE 4. Comparison of the maximum conductor temperature calculation errors of the classical model and the optimized model (cables are with different voltage levels and under different loads).

Voltage level/kV	Load/A	θ_{ce}/K	θ_{oe}/K	$\theta_c\|_{t=3h}$/K
110	1500	1.486	0.613	312.613
	2650	5.057	0.673	360.729
220	2000	4.686	0.349	329.080
	2650	8.897	0.651	359.347
500	2500	3.719	0.443	316.800
	4050	12.790	2.999	361.153

θ_{ce} - maximum absolute error of the conductor temperature obtained from the classical model with respect to that of FEM, θ_{oe} - maximum absolute error of the conductor temperature obtained from the optimized model with respect to that of FEM, and $\theta_c|_{t=3h}$ – conductor temperature at t=3h.

TABLE 5. Comparison of the averaged conductor temperature calculation errors of the classical model and the optimized model (cables are with different voltage levels and under different loads).

Voltage level/kV	Load/A	$\Delta\theta_{ce}$/K	$\Delta\theta_{oe}$/K	$\Delta\theta_{ce\text{-}oe}$/K	$\theta_c\|_{t=3h}$/K
110	1500	0.828	0.430	0.398	312.613
	2650	4.125	0.333	3.792	360.729
220	2000	4.136	0.201	3.935	329.080
	2650	7.842	0.354	7.488	359.347
500	2500	3.158	0.197	2.961	316.800
	4050	10.172	1.622	8.550	361.153

$\Delta\theta_{ce}$ - averaged absolute error of the conductor temperature obtained from the classical model with respect to that of FEM, $\Delta\theta_{oe}$ - averaged absolute error of the conductor temperature obtained from the optimized model with respect to that of FEM, and $\Delta\theta_{ce\text{-}oe}$ - difference in two models, $\Delta\theta_{ce\text{-}oe} = \Delta\theta_{ce} - \Delta\theta_{oe}$.

TABLE 6. Comparison of conductor temperature calculation error and computation time for a 500 kV cable under different insulation unit numbers.

Model	Averaged absolute error/K	Computation time/s
classical model	10.172	3.5
optimized model with n=5	6.022	3.9
optimized model with n=10	3.342	4.2
optimized model with n=15	2.462	4.5
optimized model with n=20	2.026	4.9
optimized model with n=25	1.765	5.8
optimized model with n=30	1.622	6.3
optimized model with n=40	1.406	7.0
optimized model with n=50	1.277	7.9
optimized model with n=60	1.277	9.0

The accuracy improvement of the optimized model over the classical model is also reflected on $\Delta\theta_{ce-oe}$. A large value of $\Delta\theta_{ce-oe}$ means that the accuracy improvement of the optimized model is more obvious. The above comparisons prove that the proposed optimized method for the insulation thermal model can improve the accuracy of cable dynamic rating.

It can be observed from Table 5 that when the cable conductor temperature is around 360 K, $\Delta\theta_{ce}$ and $\Delta\theta_{ce-oe}$ significantly increase with the increase of cable voltage level (i.e. insulation thickness). As an example, for 500 kV cable with insulation thickness of 43.2 mm, $\Delta\theta_{ce}$ exceeds 10 K, which is much larger than that of $\Delta\theta_{oe}$(1.622 K).

It can be also seen from Table 5 that for cables with the same voltage level, $\Delta\theta_{ce}$ and $\Delta\theta_{ce-oe}$ significantly increase with the increase of cable load. Therefore, for dynamic thermal rating of cable with high voltage level and under large load, the classical lumped thermal model may not meet the accuracy requirement. Instead, the optimized lumped thermal model can be adopted since it can trace cables' dynamic thermal characteristics.

To investigate the sensitivity of the optimized lumped thermal model on the insulation unit numbers, the optimized model was used to calculate the conductor temperatures for the 500 kV cable with different values of n. The computation time for solving the optimized model under different values of n and the corresponding calculation error $\Delta\theta_{oe}$ are presented in Table 6. The cable was under a 3-hour 4050 A step load.

It can be seen from Table 6 that there is no significant improvement in accuracy after $n > 30$. The classical lumped thermal model performed on a standard laptop computer took 3.5 seconds for temperature calculation and the error was 10.172 K; while the optimized lumped thermal model with $n = 30$ took 6.3 seconds in calculation and the error was 1.622K. Therefore, the proposed method of determining the proper number of insulation sections can attain a desirable accuracy while still keeping a high efficiency.

B. APPLICATION OF THE PROPOSED METHOD FOR CABLES

To improve the applicability of the proposed optimization method in dynamic thermal rating for cable, a work flow is implemented as shown in Fig.11. The major steps are as below.

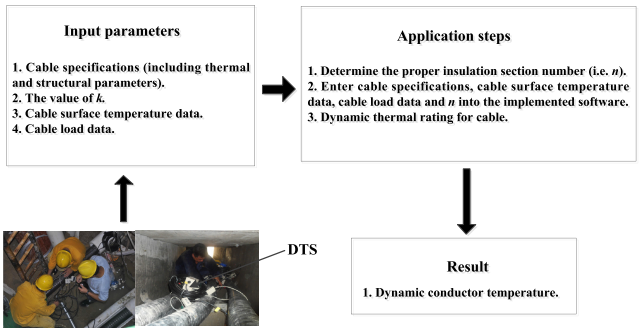

FIGURE 11. Work flow of the application of the proposed method to dynamic cable thermal rating.

1) Enter the cable structural parameters and the value of k into (33) to calculate the proper insulation section number (i.e. n).
2) Enter cable specifications, cable surface temperature data, cable load data and n into the implemented software for the optimized lumped thermal model of cable.
3) Based on the above input data, the dynamic conductor temperature can be calculated by the software.

With the advancement of sensor technology, more thermal sensors can be installed on cable in different laying modes for continuously measurement of cable surface temperature. By integrating the online monitoring data (cable surface temperature data, cable load data, and environmental weather data etc.) and the optimized transient model of cable, the accuracy of the evaluation of cable real-time operating state can be improved.

VIII. CONCLUSION

This paper treated the Van Wormer coefficient as a time-varying variable in the transient temperature calculation of the power cable. The calculation formula for the time-varying Van Wormer coefficient was derived and the approximated solution was obtained. Moreover, an error analysis of transient temperature calculation by adopting the lumped π thermal model for cable insulation as recommended by IEC 60853 was also conducted. Furthermore, a method of determining the proper number of insulation sections in the optimized lumped thermal model was proposed. The proposed method was validated with the reference to the FEM simulation. Finally, the influences of cable insulation thickness and cable loading on the improvement of temperature calculation accuracy by using the proposed method was analyzed. The results demonstrated the methods developed in this paper can improve the accuracy of cable dynamic thermal rating.

REFERENCES

[1] M. Matus *et al.*, "Identification of critical spans for monitoring systems in dynamic thermal rating," *IEEE Trans. Power Del.*, vol. 27, no. 2, pp. 1002–1009, Apr. 2012.

[2] A. Faruk and B. Yunus, "Thermal modelling and analysis of high-voltage insulated power cables under transient loads," *Comput. Appl. Eng. Educ.*, vol. 21, no. 3, pp. 516–529, Sep. 2013.
[3] R. J. Millar and M. Lehtonen, "A robust framework for cable rating and temperature monitoring," *IEEE Trans. Power Del.*, vol. 21, no. 1, pp. 313–321, Jan. 2006.
[4] R. Hoerauf, "Ampacity application considerations for underground cables," *IEEE Trans. Ind. Appl.*, vol. 52, no. 6, pp. 4638–4645, Nov./Dec. 2016.
[5] *IEC Electric Cables—Calculation of the Current Rating -Current Rating Equations (100% Load Factor) and Calculation of Losses—General*. Standard 60287-1-1, International Electrotechnical Commission, Dec. 2006.
[6] *IEC Electric Cables—Calculation of the Current Rating -Thermal Resistance— Calculation of Thermal Resistance*. Standard 60287-2-1, International Electrotechnical Commission, May 2006.
[7] R. S. Olsen, J. Holboll, and U. S. Gudmundsdóttir, "Dynamic temperature estimation and real time emergency rating of transmission cables," in *Proc. IEEE Power and Energy Society General Meeting*, San Diego, CA, USA, Jul. 2012, pp. 1–8.
[8] S.-H. Huang, W.-J. Lee, and M.-T. Kuo, "An online dynamic cable rating system for an industrial power plant in the restructured electric market," *IEEE Trans. Ind. Appl.*, vol. 43, no. 6, pp. 1449–1458, Nov./Dec. 2007.
[9] G. J. Anders, A. Napieralski, M. Zubert, and M. Orlikowski, "Advanced modeling techniques for dynamic feeder rating systems," *IEEE Trans. Ind. Appl.*, vol. 39, no. 3, pp. 619–626, May 2003.
[10] D. A. Douglass and A. Edris, "Real-time monitoring and dynamic thermal rating of power transmission circuits," *IEEE Trans. Power Del.*, vol. 11, no. 3, pp. 1407–1418, Jul. 1996.
[11] G. J. Anders and M. A. El-Kady, "Transient ratings of buried power cables. I. Historical perspective and mathematical model," *IEEE Trans. Power Del.*, vol. 7, no. 4, pp. 1724–1734, Oct. 1992.
[12] CIGRE Working Group 21.02, "Computer method for the calculation of the response of single core cables to a step function thermal transient," *Electra*, vol. 87, pp. 41–64, Mar. 1985.
[13] M. Diaz-Aguiló and F. D. León, "Introducing mutual heating effects in the ladder-type soil model for the dynamic thermal rating of underground cables," *IEEE Trans. Power Del.*, vol. 30, no. 4, pp. 1958–1964, Aug. 2015.
[14] G. Mazzanti, "Analysis of the combined effects of load cycling, thermal transients, and electrothermal stress on life expectancy of high-voltage AC cables," *IEEE Trans. Power Del.*, vol. 22, no. 4, pp. 2000–2009, Oct. 2007.
[15] G. Mazzanti and M. Marzinotto, "More insight into the effects of load cycles and electrothermal stress on HVDC extruded cable reliability in the prequalification test," in *Proc. IEEE Power Energy Soc. Gen. Meeting*, Vancouver, BC, Canada, Jul. 2013, pp. 1–5.
[16] F. C. Van Wormer, "An improved approximate technique for calculating cable temperature transients," *Trans. Amer. Inst. Elect. Eng. III, Power App. Syst.*, vol. 74, no. 3, pp. 277–281, Jan. 1955.
[17] G. Jerzy and Z. Marek, "The simplified method for transient thermal field analysis in a polymeric DC cable," *Elect. Eng.*, vol. 93, no. 4, pp. 209–216, Dec. 2011.
[18] *IEC Electric Cables—Calculation of the Cyclic and Emergency Current Rating of Cables -Cyclic Rating of Cables Greater Than 18/30(36) kV and Emergency Ratings for Cables of all Voltages*. Standard 60853-2, International Electrotecnical Commission, Jul. 1989.
[19] K. Dardan, P. Bojan, K. Jelena, J. Milena, M. Miloš, and K. Ivan, "Controlling the thermal environment of underground cable lines using the pavement surface radiation properties," *IET Gener., Transmiss. Distrib.*, vol. 12, no. 12, pp. 2968–2976, Jul. 2018.
[20] H. D. Baehr and K. Stephan, *Heat and Mass Transfer*. Berlin, Germany: Springer, 2006.
[21] R. Olsen, G. J. Anders, J. Holboell, and U. S. Gudmundsdottir, "Modelling of dynamic transmission cable temperature considering soil-specific heat, thermal resistivity, and precipitation," *IEEE Trans. Power Del.*, vol. 28, no. 3, pp. 1909–1917, Jul. 2013.
[22] G. J. Anders, *Rating of Electric Power Cables*. New York, NY, USA: McGraw-Hill, 1997.
[23] M. Diaz-Aguiló, F. D. León, S. Jazebi, and M. Terracciano, "Ladder-type soil model for dynamic thermal rating of underground power cables," *IEEE Power Energy Technol. Syst. J.*, vol. 1, pp. 21–30, Dec. 2014.
[24] Y. Liang, Q. Liu, H. Sun, and Y. Li, "Cable load dynamic adjustment based on surface temperature and thermal circuit model," in *Proc. Int. Conf. Condition Monit. Diagnosis (CMD)*, Beijing, China, Apr. 2008, pp. 705–708.

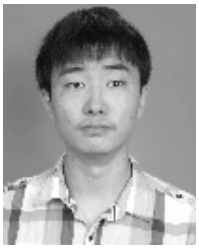

PENG-YU WANG received the B.Sc. Eng. degree in electrical engineering from the South China University of Technology, Guangzhou, China, in 2016, where he is currently pursuing the Ph.D. degree.

His research interests include ampacity assessment and fault diagnosis of power cable.

HUI MA received the B.Eng. and M.Eng. degrees from Xi'an Jiaotong University, Xi'an, China, in 1991 and 1994, respectively, the M.Eng. (by research) degree from Nanyang Technological University, Singapore, in 1998, and the Ph.D. degree from The University of Adelaide, Adelaide, SA, Australia, in 2008, all in electrical engineering. From 1994 to 1995, he was a Researcher with Xi'an Jiaotong University. From 1997 to 1999, he was a Firmware Development Engineer with CET Technologies Pte. Ltd., Singapore. He was a Research Engineer with the Singapore Institute of Manufacturing Technology, from 1999 to 2003. He is currently a Lecturer with the School of Information Technology and Electrical Engineering, The University of Queensland, Brisbane, QLD, Australia, where he spent many years on research and development. His research interests include industrial informatics, condition monitoring and diagnosis, power systems, wireless sensor networks, and sensor signal processing.

GANG LIU received the B.Eng., M.Eng., and Ph.D. degrees in electrical engineering from Xi'an Jiaotong University, Xi'an, China, in 1991, 1994, and 1998, respectively. He is currently an Associate Professor with the School of Electric Power, South China University of Technology, Guangzhou, China. His research interests include ampacity assessment and fault diagnosis of electrical equipments and lightning protection of transmission line.

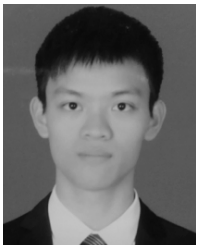

ZHUO-ZHAN HAN received the B.Sc. Eng. degree in electrical engineering from the South China University of Technology, Guangzhou, China, in 2016, where he is currently pursuing the M.Eng. degree.

His research interests include ampacity assessment and fault diagnosis of power cable.

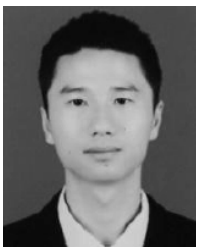

DE-MING GUO received the B.Sc. Eng. degree in electrical engineering from South China Agricultural University, Guangzhou, China, in 2016. He is currently pursuing the M.Eng. degree in electrical engineering from the South China University of Technology, Guangzhou.

His research interests include ampacity assessment and fault diagnosis of overhead transmission line.

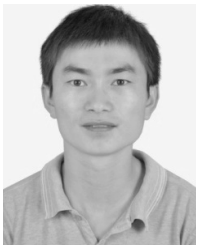

TAO XU received the B.Eng. degree in electrical engineering from Hunan University, Changsha, China, in 2007, and the M.Eng. degree in electrical engineering from the South China University of Technology, Guangzhou, China, in 2011. He is currently an Engineer with Guangzhou Power Supply Co., Ltd., Guangzhou. His research interest includes operation and maintenance of cables.

LONG-YUN KANG received the B.Eng. degree from Yanbian University, Yanji, China, in 1982, and the M.Eng. and Ph.D. degrees from Kyoto University, Kyoto, Japan, in 1996 and 1999, respectively.

He is currently a Professor with the School of Electric Power, South China University of Technology, Guangzhou, China. His research interests include battery energy storage technology and motor control technology.